Simplified estimation of ray-path mirroring height for HF radiowaves reflected from the ionospheric F-region

M. Lockwood, B.Sc., Ph.D.

Indexing terms: *Radiowave propagation, Ionospheric propagation*

Abstract: From Milsom's equations, which describe the geometry of ray-path hops reflected from the ionospheric F-layer, algorithms for the simplified estimation of mirror-reflection height are developed. These allow for hop length and the effects of variations in underlying ionisation (via the ratio of the F2- and E-layer critical frequencies) and F2-layer peak height (via the M(3000)F2-factor). Separate algorithms are presented which are applicable to a range of signal frequencies about the FOT and to propagation at the MUF. The accuracies and complexities of the algorithms are compared with those inherent in the use of a procedure based on an equation developed by Shimazaki.

List of principal symbols

a = $(M(3000)_i^{-1} - 0.24)$ or 0.04, whichever is the larger
B = slope of the variation of s with $M(3000)_i^{-1}$ for $r = 0.85$
B_1 = slope of the variation of s_1 with $M(3000)_o^{-1.5}$ for $r = 1$
c = intercept of linear fit to h_T variation with D for $r = 0.85$
c_1 = intercept of linear fit to h_T variation with D for $r = 1$
D = ground range of a single hop
D_{max} = maximum range for a single hop
f = signal frequency
f_e = equivalent frequency for which $h_T = hm$ at oblique incidence
fo = critical frequency for layer
foE = critical frequency of E-layer
foF2 = critical frequency of F2-layer
FOT = optimum transmission frequency (= 0.85 MUF)
h' = virtual-reflection height for vertical incidence
h_p = Shimazaki's estimate of hm
hm = height of layer peak
hmE = height of E-layer peak
hmF2 = height of F2-layer peak
h_T = mirror-reflection height for oblique incidence
k = curved-Earth correction factor
$M(D)$F2 = M-factor for single hop, reflected by the F2-layer to a range D km (= MUF/foF2)
$M(3000)_i$ = M(3000)F2-factor scaled from synthesised ionogram
$M(3000)_o$ = M(3000)F2-factor derived from oblique propagation equations
MUF = basic maximum usable frequency
r = ratio of signal frequency to MUF (f/MUF)
R_E = radius of curvature of Earth's surface
s = slope of linear fit to h_T variation with D for $r = 0.85$
s_1 = slope of linear fit to h_T variation with D for $r = 1$
w = ground range as a fraction of its maximum value (D/D_{max})
x = ratio of F2- and E-layer critical frequencies (foF2/foE)
ym = layer semithickness
ymE = E-layer semithickness
ymF2 = F2-layer semithickness
α = slope of variation of c with $M(3000)_i^{-1}$ for $r = 0.85$
α_1 = slope of variation of c_1 with $M(3000)_o^{-1}$ for $r = 1$
β_0 = elevation angle of ray hop
δ = error in simplified estimate of h_T
δ_m = maximum of δ
Δ = correction to linear variation of h_T with D for $r = 1$
ε = average of δ
ϕ = function of f and fo, defined by Booker and Seaton [5]

Paper 3007F (E8, E11), first received 6th May and in final form 12th December 1983
The author is with the Rutherford Appleton Laboratory, Chilton, Didcot, Oxford OX11 0QX

1 Introduction

The mirror-reflection height is that height at which an equivalent plane mirror would have to be placed to reflect unrefracted waves with the same elevation angles at the receiver and transmitter as for the real ionosphere. It is a convenient concept in characterising the geometry of an ionospherically supported ray hop for use in propagation predictions, in the evaluation of antenna gains, path loss and group path delay [1, 2].

For propagation modes reflected from the F2-layer, the mirror-reflection height is difficult to estimate accurately; in several of the larger HF propagation prediction procedures it is calculated iteratively [1, 2]; alternatively equations based on some mean reference model ionosphere can be employed [3]. The advantages of the iterative procedures are that the effects of spatial variations in the height of the reflecting layer and changes in underlying ionisation can be taken into account; also that the evaluation can be continued until the required accuracy is achieved. For many applications, however, the computation must be completed in a restricted period of time or may be based on ionospheric data of accuracy which does not justify rigorous solution. In these cases the mean-ionosphere approach is favoured.

Reflection by a spherically curved parabolic model layer was initially considered by Appleton and Beynon [4]. From their equations Booker and Seaton [5] derived the relationship for the virtual-reflection height, of a signal frequency f at vertical incidence:

$$h' = hm + ym\phi(f/fo) \tag{1}$$

where hm, ym and fo are the layer peak height, semithickness and critical frequency, respectively. The function ϕ is zero when f equals $0.834fo$; hence, hm equals h' at this frequency. From Martyn's equivalent path theorem, generalised to allow for the Earth's curvature (radius = R_E), hm equals the mirror-reflection height, h_T, for an equivalent, oblique-incidence frequency [6]:

$$f_e = \frac{0.834fo}{k} \sin\left(\beta_0 + \frac{D}{2R_E}\right) \tag{2}$$

where β_0 is the hop elevation angle and the curved-Earth correction factor, k, is 1.0 for short hop length, D, and about 1.2 for large D. Shimazaki [3] derived a simple empirical expression for an approximation to hm, h_p, using data from a global network of ionosondes:

$$hm \cong h_p = \frac{1490}{M(3000)\mathrm{F2}} - 176 \text{ km} \tag{3}$$

the $M(3000)$F2-factor being scaled routinely from ionograms. Subsequently, this equation has often been used to give estimates for h_T with the inherent assumption that the signal frequency is approximately equal to $f_e(D)$; an application which Shimazaki had not intended. Amended coefficients were suggested by Wright and McDuffie [7]; however, eqn. 3 remains in use today as an approximate method of determining mirror-reflection heights [8].

The Shimazaki formula (eqn. 3) is based on a single parabolic reflecting layer. Hence, for F2-layer propagation, the effects of underlying ionisation beneath the F2-layer are not accounted for. A more complete model ionospheric profile, with variable amounts of underlying ionisation, has been proposed by Bradley and Dudeney [9], consisting of a combination of linear and parabolic segments to represent the E-, F1- and F2-regions. To allow exact analytic solution of ray-path parameters, Milsom [10] has fitted quasilinear and quasiparabolic segments to give a close approximation to the Bradley–Dudeney profile. In a previous paper, the present author listed Milsom's equations for the ground range and group path of a hop reflected by such a model ionosphere, and used them to develop an algorithm for simplified, noniterative estimation of basic maximum usable frequency [11]. Allowance was made for variations in both underlying ionisation and F2 peak height. In this paper complementary algorithms for estimation of mirror-reflection height are derived and assessed.

2 Model parameters used in the study

The general form of the Milsom approximation to the Bradley–Dudeney model ionospheric profile is demonstrated by Fig. 1. The E-layer peak height, hmE, and semithickness, ymE, are fixed at 110 km and 20 km, respectively; hence, the entire profile is characterised by the remaining four independent variables, namely the E- and F2-layer critical frequencies, foE and foF2, and the F2-layer peak height and semithickness, hmF2 and ymF2. Bradley and Dudeney [8] concluded that, in practice, the ratio hmF2/ymF2 generally lies between 2.0 and 5.0. Here, as in the previous study of basic maximum usable frequency (MUF), a fixed ratio of 3.5 is adopted, thereby reducing the number of independent ionospheric variables to three.

For a given such ionospheric profile, h_T depends on these three ionospheric parameters and on the signal frequency f, and the ground range, D. The Milsom equations

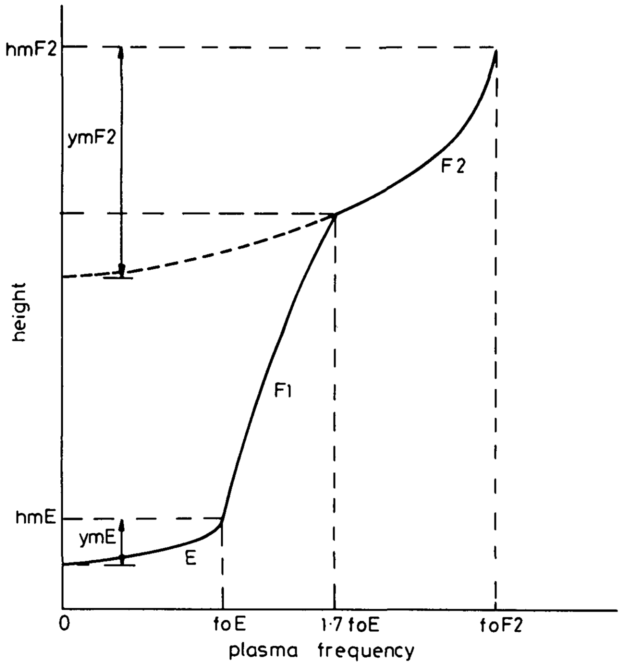

Fig. 1 *Fit of quasiparabolic and quasilinear segments to the Bradley–Dudeney model profile*

show that h_T has the functional form:

$$h_T = h_T(hm\mathrm{F2}, x, fo\mathrm{E}/f, fo\mathrm{F2}/f, D) \tag{4}$$

where x is the ratio (foF2/foE). In this paper use is made of a parameter r, the ratio (f/MUF). In Reference 11 it is shown that:

$$f = rfo\mathrm{F2}M(x, hm\mathrm{F2}, D) \tag{5}$$

Hence from eqns. 4 and 5:

$$h_T = h_T(hm\mathrm{F2}, x, r, D) \tag{6}$$

A range of hmF2 between 250 km and 500 km is considered here, and six values, 50 km apart, are found to be adequate to characterise the behaviour of h_T. The value of h_T is very dependent on x near 1.7, which is the limit of applicability of the model, but is more slowly varying at large x: x of 10, 5, 3.33, 2.5, 2.22, 2.08 and 2.0 are examined. The algorithms devised here are not, therefore, designed for use with x less than 1.95. The greatly increased complexity required to evaluate h_T for any lower x is not considered justified by the model approximations used. Cases of low x are rare and are predominately found for the daytime high-latitude ionosphere in winter at sunspot minimum.

The variation of h_T with range, D, was then studied for each model ionosphere profile with signal frequency equal to various fractions, r, of the basic MUF.

3 Calculation of mirror-reflection height for model ionospheric profiles

For each of the 42 model ionospheric profiles, an ordinary-wave ionogram trace was synthesised using the group-path equations [11] and an $M(3000)$F2-value was scaled using the standard URSI slider. The value of MUF for a fixed D was calculated iteratively by the procedure given by Lockwood [11] and a value of h_T then calculated for that D and a fixed r (f/MUF) by iterating the elevation angle, β_0. In this way $h_T(D)$ curves were calculated for various r and for each of the model profiles.

Fig. 2 shows a set of $h_T(D)$ curves for various values of r with x of 3.33 and hmF2 equal to 250 km and 500 km. The

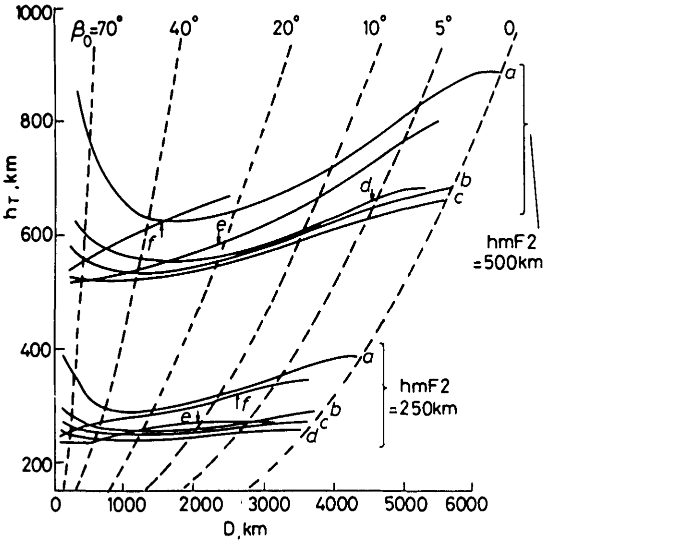

Fig. 2 *Mirror-reflection height, h_T, as a function of distance, D, with hmF2 of 250 km and 500 km, and x = 3.33*

a $r = 1.0$ *d* $r = 0.8$
b $r = 0.95$ *e* $r = 0.7$
c $r = 0.9$ *f* $r = 0.6$
– – – – constant elevation angle, β_0

important range of r between 0.6 and 1.0 is considered for both these two model profiles. It can be seen that, over a large part of this range of r, h_T at a fixed D is only weakly dependent on r (for $r = 0.8 - 0.95$ when hmF2 = 500 km and for $r = 0.7 - 0.95$ when hmF2 = 250 km, except at the shortest ranges). In every case where $r \geqslant 0.7$, h_T is greatest at all D when r is unity; it is much greater than for the lower r at the smallest and largest distances.

The variations of h_T with x for hmF2 of 250 km and 500 km are illustrated by Fig. 3 for $r = 1.0$ and by Fig. 4 for $r = 0.85$. The h_T is most dependent on x near the lower limit of 2.0, and increasing the underlying ionisation (decreased x) results in an h_T rise which is greater at large D and large hmF2.

The variation of h_T with hmF2 is considerably more regular than that with r or x, as is demonstrated by Fig. 5

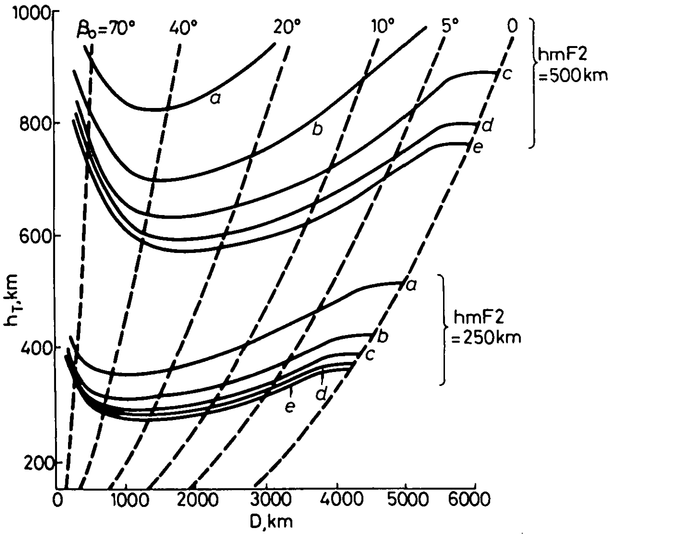

Fig. 3 *Mirror-reflection height, h_T, as a function of distance, D, for r = 1.0 with hmF2 of 250 km and 500 km*

a $x = 2.0$ *d* $x = 5.0$
b $x = 2.5$ *e* $x = 10.0$
c $x = 3.33$
– – – – constant elevation angle, β_0

for $r = 0.85$ and $x = 3.33$. At a fixed D, h_T increases approximately linearly with hmF2. Note that at low hmF2

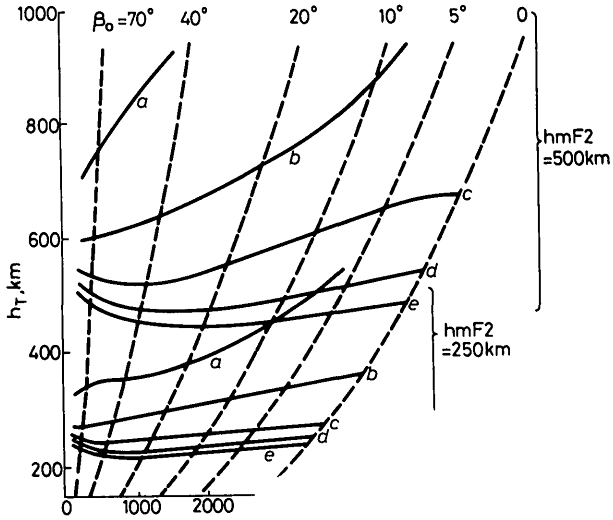

Fig. 4 *Mirror-reflection height, h_T, as a function of distance, D, for r = 0.85 with hm F2 of 250 km and 500 km*

a $x = 2.0$ *d* $x = 5.0$
b $x = 2.5$ *e* $x = 10.0$
c $x = 3.33$
– – – – constant elevation angle, β_0

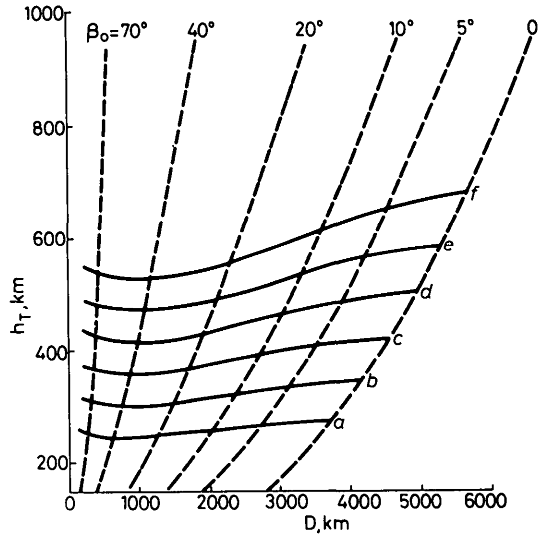

Fig. 5 *Mirror-reflection height, h_T, as a function of distance, D, for r = 0.85 and x = 3.33*

a hmF2 = 250 km *d* hmF2 = 400 km
b hmF2 = 300 km *e* hmF2 = 450 km
c hmF2 = 350 km *f* hmF2 = 500 km
– – – – constant elevation angle, β_0

($\lesssim$350 km), high x ($\gtrsim$3.3) and f = FOT, h_T equals hmF2 to within 10%.

4 Algorithms for rapid evaluation of mirror-reflection height

Inspection of sets of $h_T(D)$ curves like that shown in Fig. 2 reveals that h_T is a complicated function of r. However, for the range of r between about 0.75 and 0.95, h_T is approximately a linear function of D; hence, this range can be characterised with relative simplicity. As the majority of HF communication circuits employ this range of r (by operating as close as interference permits to the optimum transmission frequency, FOT, defined by f = FOT when $r = 0.85$), such a simplification should have wide applications.

A second requirement for prediction of mirror-reflection height exists at the basic MUF ($r = 1.0$). Many prediction procedures require this information in order that propagation losses at frequencies above the monthly median basic MUF can be assessed.

In the following Sections algorithms are developed for these two ranges of r.

4.1 Algorithms applicable to a range of signal frequencies about the FOT

Fig. 2 demonstrates that, at all but the shortest ranges, h_T can be described by the linear form when $0.75 < r < 0.95$:

$$h_T = sD + c \tag{7}$$

Linear regression lines were fitted to all $h_T(D)$ curves for $r = 0.85$ ($f =$ FOT). The slopes, s, of these regression lines are plotted in Fig. 6 as a function of the inverse of the

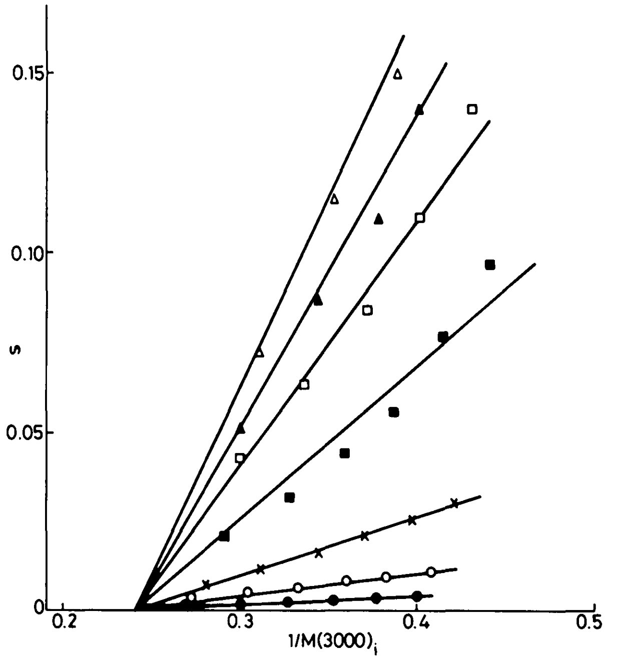

Fig. 6 *Slope of regression lines, s, as a function of the inverse of M(3000)$_i$*

△ $x = 2.0$ × $x = 3.33$
▲ $x = 2.08$ ○ $x = 5.0$
□ $x = 2.22$ ● $x = 10.0$
■ $x = 2.5$

M(3000)F2-factor scaled from the synthesised ionogram; this M-factor is referred to here as $M(3000)_i$ to be consistent with Reference 11. For a fixed value of x, s is roughly inversely proportional to $M(3000)_i$ and is approximately given by:

$$s = \left(\frac{1}{M(3000)_i} - 0.24\right)B \qquad \text{for } M(3000)_i \leqslant 3.57 \tag{8}$$

It was found that use of eqn. 8 for $M(3000)_i$ greater than 3.57 gave large errors in h_T at large x and D. This problem was overcome by the introduction of the condition:

$$s = 0.04B \qquad M(3000)_i > 3.57 \tag{9}$$

The slopes of the fitted lines shown in Fig. 6, B, vary linearly with the inverse of the fourth power of x:

$$B = 0.03 + 14.0/x^4 \tag{10}$$

The intercept, c, of the regression lines is also approximately inversely proportional to $M(3000)_i$ at fixed x (see Fig. 7), and straight lines which pass through the point ($c = 358$, $1/M(3000)_i = 0.35$) can be adopted. Least-squares fits to these lines give the values of their slope, α, shown in Fig. 8 as a function of x. The solid curve satisfies

$$\alpha = 1880 - 32\,000/x^5 \tag{11}$$

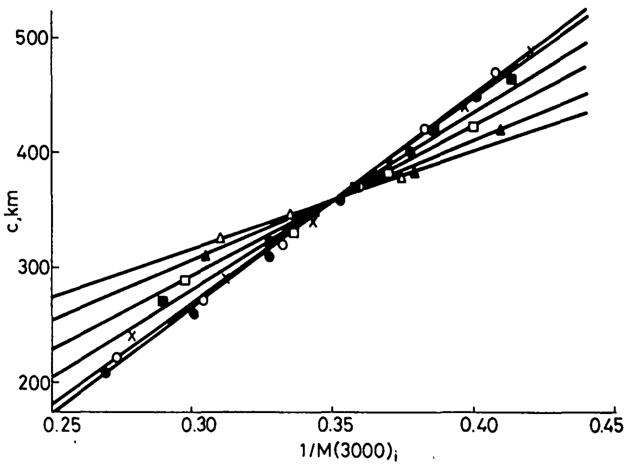

Fig. 7 *Intercept of regression lines, c, as a function of the inverse of M(3000)$_i$*

△ $x = 2.0$ × $x = 3.33$
▲ $x = 2.08$ ○ $x = 5.0$
□ $x = 2.22$ ● $x = 10.0$
■ $x = 2.5$

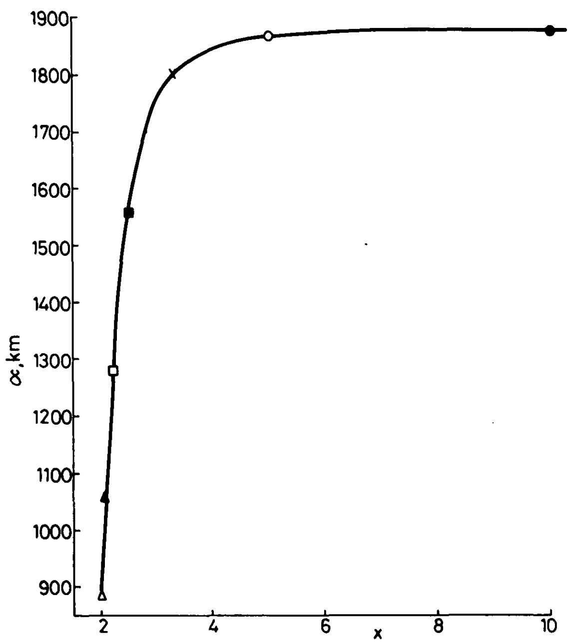

Fig. 8 *Slope of fitted lines in Fig. 7, α, as a function of x with an approximate polynomial fit*

△ $x = 2.0$ × $x = 3.33$
▲ $x = 2.08$ ○ $x = 5.0$
□ $x = 2.22$ ● $x = 10.0$
■ $x = 2.5$

and c is given by:

$$c = 358 + \alpha\left(\frac{1}{M(3000)_i} - 0.35\right) \tag{12}$$

Eqns. 7–12 can be combined into the equation:

$$h_T = 358 - (11 - 100a)\left(18.8 - \frac{320}{x^5}\right) + aD\left(0.03 + \frac{14}{x^4}\right) \text{ km} \tag{13}$$

where $a = (1/M(3000)_i) - 0.24$, or 0.04 whichever is the larger. The full eqn. 13 allows simple and rapid evaluation of h_T, the accuracy of which is assessed in Section 5.

Comparison with eqn. 2 shows that the above full equation is considerably more complex than the Shimazaki equation which is widely used to predict h_T. However, the full equation can be simplified, with some loss of accuracy, to separate equations for night and day by adopting representative mean values of x:

$$\textit{night } (x \sim 10) \qquad h_T = \frac{1880}{M(3000)_i} - 300 \text{ km} \tag{14}$$

$$\textit{day } (x \sim 3) \qquad h_T = 160 + (0.143D + 1800) \times \left\{\frac{1}{M(3000)_i} - 0.24\right\} \text{ km} \tag{15}$$

The night equation has the same form as that of Shimazaki, with new values for the constants: the increase in h_T with D is neglected in both expressions. On the other hand, Fig. 4 demonstrates that this increase needs to be included for the x values common in the dayside ionosphere ($x \lesssim 3$), and accordingly the day equation contains an additional distance term. The accuracy of the simplified eqns. 14 and 15 is also assessed in Section 5.

4.2 Algorithm applicable to a signal frequency equal to the basic MUF

Fig. 3 shows that the general form of the $h_T(D)$ curves for $r = 1.0$ cannot be approximated by a single linear relationship as was possible for the $r = 0.85$ curves. Figs. 9 and 10

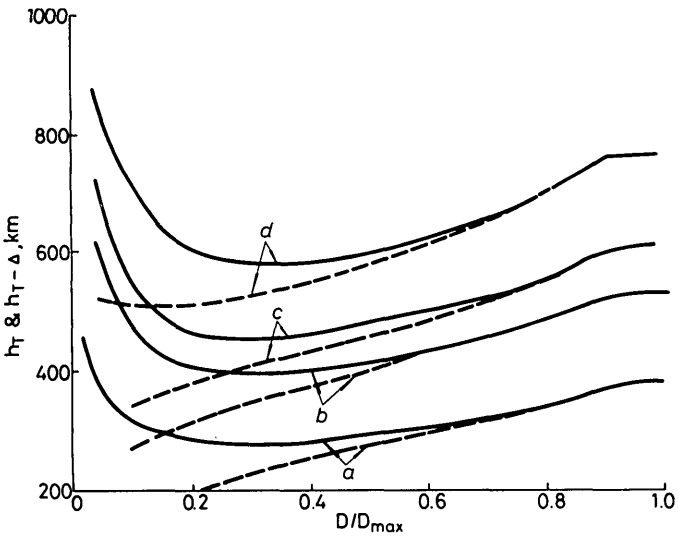

Fig. 9 *h_T and $h_T - \Delta$ as a function of D/D_{max} for $x = 10.0$*
a *hm*F2 = 250 km
b *hm*F2 = 350 km
c *hm*F2 = 400 km
d *hm*F2 = 500 km
- - - - $h_T - \Delta$
——— h_T

demonstrate that the increase of h_T with decreasing D at the lowest distances can be accounted for by the use of a single correction term Δ, chosen such that $(h_T - \Delta)$ has a near-linear variation with (D/D_{max}), where D_{max} is the maximum range (corresponding to zero elevation of the ray path, β_0) and is given by eqns. 18 and 19 of Reference 11. Curves for h_T (solid line) and $(h_T - \Delta)$ (broken line) are given for *hm*F2 of 250, 350, 400 and 500 km with x of 10.0 in Fig. 9 and with x of 2.2 in Fig. 10.

The form for Δ used in Figs. 9 and 10 is:

$$\Delta = 23\left(\frac{1}{w} - 1\right) \tag{16}$$

where w equals (D/D_{max}). Hence, h_T can be approximated by:

$$\begin{aligned} h_T &= s_1 w + c_1 + \Delta \qquad & w \leqslant 0.95 \\ h_T &= [h_T]_{w=0.95} \qquad & w > 0.95 \end{aligned} \tag{17}$$

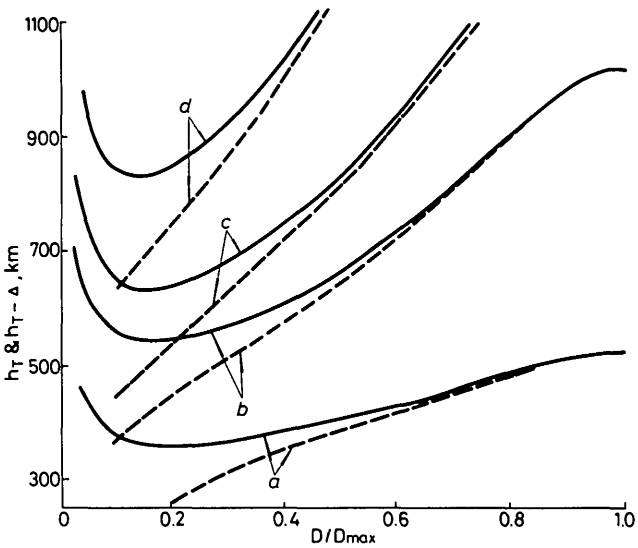

Fig. 10 *h_T and $h_T - \Delta$ as a function of D/D_{max} for $x = 2.22$*
a *hm*F2 = 250 km
b *hm*F2 = 350 km
c *hm*F2 = 400 km
d *hm*F2 = 500 km
- - - - $h_T - \Delta$
——— h_T

The second expression allows for the flattening of the $h_T(D)$ curves as D approaches D_{max}.

The intercept c_1 can be fitted in the same way as c in the preceding Section, giving expressions of the same form as eqns. 11 and 12 but with different constants:

$$c_1 = 35 + \alpha_1 \left\{\frac{1}{M(3000)_o} - 0.225\right\} \tag{18}$$

where

$$\alpha_1 = 1785 - 4000/x^3 \tag{19}$$

and $M(3000)_o$ is the ordinary-wave M-factor from the iteration of ray-path solutions for a range of 300 km. In general, this differs from $M(3000)_i$ and is derived in the MUF algorithm procedure given in Reference 10. The slope s_1 varies linearly with $M(3000)_o$ to the power -1.5:

$$s_1 = 230 + B_1(M(3000)_o^{-1.5} - 0.14) \tag{20}$$

and

$$B_1 = 325 + 6.4 \times 10^4/x^{3.8} \tag{21}$$

Eqns. 16–21 can be used to evaluate h_T for $f =$ MUF at a given D, in conjunction with the values for $M(3000)_o$ and D_{max} obtained in the evaluation of MUF by the simplified algorithm by Lockwood [11]. The accuracy of the h_T values is assessed in Section 5.2.

5 Accuracy of mirror-reflection height algorithms

The accuracy of the algorithms presented in Sections 4.1 and 4.2 are assessed by comparing the predicted mirror-reflection height, for a given range and ionospheric profile, with results of the full calculation using the Milsom equations. The error as a percentage of the correct value, δ, is evaluated; positive values of δ representing overestimates of mirror-reflection height.

5.1 Accuracy of predictions for the range of r between 0.75 and 0.95

Fig. 11 plots simplified predictions using eqn. 13 (broken lines) and fully calculated values (solid lines) for the

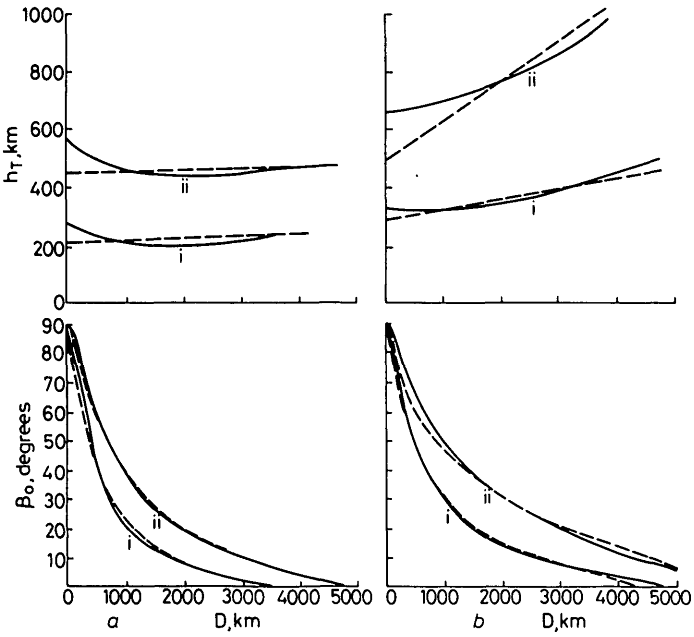

Fig. 11 *Fully calculated values and approximate estimates given by eqn. 13 (r = 0.85) for the mirror-reflection height, h_T, and elevation angle, β_0, as a function of distance, D*

a $x = 10.0$
b $x = 2.22$
i *hm*F2 = 250 km ii *hm*F2 = 500 km
——— calculated values
- - - - estimates

mirror-reflection height, h_T, and ray-path elevation angles, β_0, for x of 10.0 and 2.22, and *hm*F2 of 250 km and 500 km. It can be seen that there is a tendency to underestimate h_T and β_0 at low D for this r of 0.85. Other results not presented reveal that the tendency is smaller at low r, but is larger at greater r, and increases with increasing *hm*F2 and decreasing x. Although these cases give quite large fractional errors in h_T for near-vertical propagation, the associated errors in β_0 are small. Table 1 lists the

Table 1: Largest percentage errors (positive values are overestimates) in using eqn. 13, δm, for r of 0.75, 0.80, 0.85, 0.90 and 0.95

	*hm*F2, km							
x		10.0	5.0	3.33	2.5	2.22	2.08	2.0
D = 1000 km								
	250	4.9	1.8	−3.8	−2.6	−2.7	−3.9	−4.3
	300	2.4	1.1	−0.9	−0.5	−2.4	−4.3	−5.0
	350	3.6	2.3	1.5	−0.5	−3.4	−7.0	−10.9
	400	3.6	2.7	0.2	−2.6	−4.7	−8.2	—
	450	3.1	0.6	−0.2	−3.7	−7.9	−9.1	—
	500	2.1	0.3	−2.7	−5.7	−8.5	—	—
D = 3000 km								
	250	0.0	−2.9	−6.4	−3.9	−3.8	−3.5	−2.3
	300	−0.8	−2.3	−3.4	0.1	1.9	5.0	8.0
	350	2.0	0.0	−0.6	1.8	5.9	8.6	10.6
	400	2.5	0.9	−1.1	1.5	6.5	9.7	—
	450	3.7	−0.4	−1.0	1.6	7.1	10.6	—
	500	3.5	−0.3	−2.0	1.9	—	—	—

largest error, δ_m, with r of 0.75–0.95 for each of the 42 model ionospheric profiles for which ray-tracing solutions are possible. The errors for D of 3000 km were largely independent of r, whereas those for 1000 km are largest for the $r = 0.95$ case and generally decrease with decreasing r. Errors are less than 5% in all but one case: when $x \geqslant 2.5$. For the full range of x considered here (2.0–10.0), values are accurate to within about 10%; worst errors arising from high D, low x and high *hm*F2 cases. For distances near 1000 km, eqn. 13 tends to overestimate h_T at high x and underestimate at low x; for the greater ranges it tends to overestimate at low and high x and underestimates for intermediate x. At the shortest ranges eqn. 13 gives underestimates, particularly for the larger r.

Table 2 gives the equivalent errors to those in Table 1 for mirror-height evaluation using the Shimazaki eqn. 2.

Table 2: Largest percentage errors (positive values are overestimates) in using the Shimazaki eqn. 3, δm for r of 0.75, 0.80, 0.85, 0.90 and 0.95

	*hm*F2, km							
x		10.0	5.0	3.33	2.5	2.22	2.08	2.0
D = 1000 km								
	250	4.0	2.5	−1.6	−9.5	−17.0	−23.0	−25.5
	300	3.2	1.5	−4.0	−11.6	−19.3	−25.5	−29.5
	350	1.0	−0.9	−5.6	−15.2	−21.6	−27.9	−32.1
	400	−2.0	−3.7	−8.5	−18.1	−23.7	−31.3	—
	450	−4.0	−7.1	−11.3	−21.0	−26.6	−35.1	—
	500	−6.8	−9.0	−14.1	−22.3	−28.7	—	—
D = 3000 km								
	250	−2.0	−3.7	−9.1	−21.4	−30.7	−40.6	−42.7
	300	−2.4	−4.1	−12.5	−25.4	−32.1	−41.3	−44.1
	350	−3.0	−5.9	−14.7	−28.5	−35.5	−41.8	−45.2
	400	−4.6	−7.9	−17.5	−31.2	−36.2	−43.3	—
	450	−5.1	−11.2	−19.6	−32.7	−36.6	−44.6	—
	500	−6.4	−12.6	−21.6	−33.8	—	—	—

Because eqn. 2 contains no allowance for the increase of h_T with D, it tends to seriously underestimate, particularly at large D. Errors are similar to those given in Table 1 at $x = 10$ but rise to over 30% for $x \geqslant 2.5$ and 45% for $x \geqslant 2.0$.

The overall behaviour of the errors for the simplified equations are compared in Fig. 12, which shows the means of the moduli of the error deviations δ, averaged over all six *hm*F2 and as a function of $x(\varepsilon = \langle|\delta|\rangle)$. The dotted curve gives the error for the full eqn. 13 and the dashed curve that for the Shimazaki equation. The former gives mean errors which are less than 5% at all but the lowest x, the latter is seriously in error (underestimates) at low x, particularly for the greater range. The solid curve shows the mean errors for the night eqn. 14 and the broken curve those for the day eqn. 15; both of which tend to underestimate h_T at low x in the same way as for the Shimazaki equation. The day equation gives smaller errors than the Shimazaki, at all x below 5, and smaller errors than the night equation for x below about 4.5. Hence, if in the interests of method simplicity eqns. 14 and 15 are used instead

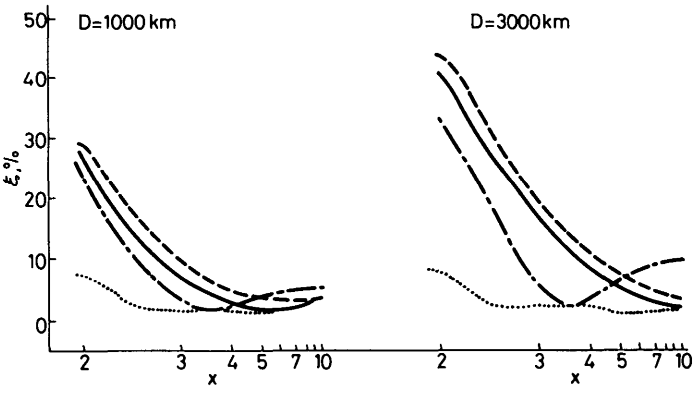

Fig. 12 *Mean of moduli of δ, ξ, as a function of x for prediction by various simplified equations*

- - - - Shimazaki (eqn. 3)
——— night (eqn. 14)
—·—· day (eqn. 15)
.... full (eqn. 13)

of eqn. 13, the day equation should be applied when $x \leqslant 4.5$ and the night equation at all greater x. Note that the errors for the night equation are slightly smaller than those for Shimazaki at all x; hence, the coefficients given in eqn. 14 are preferable if the simplest form of a single equation for h_T is required. Fig. 13 demonstrates that the day

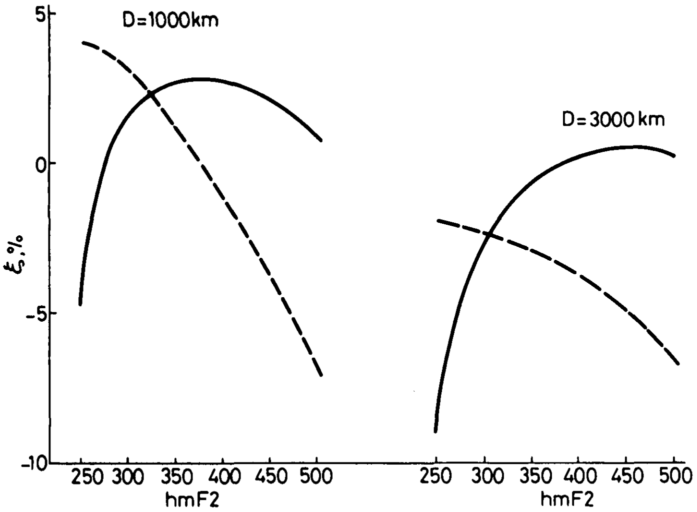

Fig. 13 *Mean error, ξ, as a function of hmF2 for $x = 10.0$ given by the day equation and by Shimazaki*

——— day equation
- - - - Shimazaki equation

equation also gives a more desirable variation in errors with *hm*F2. The values of δ are shown for x of 10 and as a function of *hm*F2; the dashed and solid curves are for the Shimazaki and high equations, respectively. The high-x case is most applicable under night conditions when *hm*F2 is generally high. Fig. 13 shows that the night equation is more accurate for high *hm*F2. The Shimazaki equation is only more accurate for high x and high *hm*F2, which is a relatively rare combination.

5.2 Accuracy of values for r of 1.0

Fig. 14 plots fully calculated h_T and β_0 (solid curves) and values from the simplified algorithm (eqns. 13–18). Because of the large gradient of the curves at short distance and the simplicity of the correction term Δ (eqn. 13), large errors in h_T can arise for distances below 1000 km; Fig. 14 demonstrates that errors in β_0 are still small. Table 3 gives the

Table 3: Percentage error (positive values are overestimates) in using eqns. 16–21, δ, for unity *r*

	*hm*F2, km							
x		10.0	5.0	3.3	2.5	2.22	2.08	2.0
D = 1000 km								
	250	1.9	1.1	−1.0	−0.1	0.7	−4.8	−3.1
	300	2.7	1.5	0.6	0.7	1.5	3.4	1.9
	350	4.4	3.1	1.7	1.9	4.5	8.2	7.6
	400	2.7	2.3	1.8	5.0	11.1	2.0	—
	450	1.2	0.9	−3.2	4.5	8.3	2.0	—
	500	−1.5	−3.1	−5.4	4.3	7.0	—	—
D = 3000 km								
	250	1.9	0.5	−0.8	−3.4	14.3	14.1	10.1
	300	3.0	2.7	1.1	0.7	15.3	19.7	19.6
	350	4.5	4.0	3.8	3.9	15.9	21.0	31.9
	400	4.1	4.3	4.2	5.7	17.8	17.6	—
	450	3.3	3.7	4.6	5.5	21.4	19.0	—
	500	2.9	1.3	−0.2	4.3	—	—	—

percentage errors ε, for D of 1000 and 3000 km. Errors are always less than 6% for $x \geqslant 2.5$; at lower x errors are larger, rising to over 30% for $x = 2.0$ at the larger distance because of slight deviations of $(h_T - \Delta)$ from a linear dependence on D/D_{max}, particularly for high *hm*F2 and low x. The algorithm would be significantly more complex if allowance were to be made for this effect.

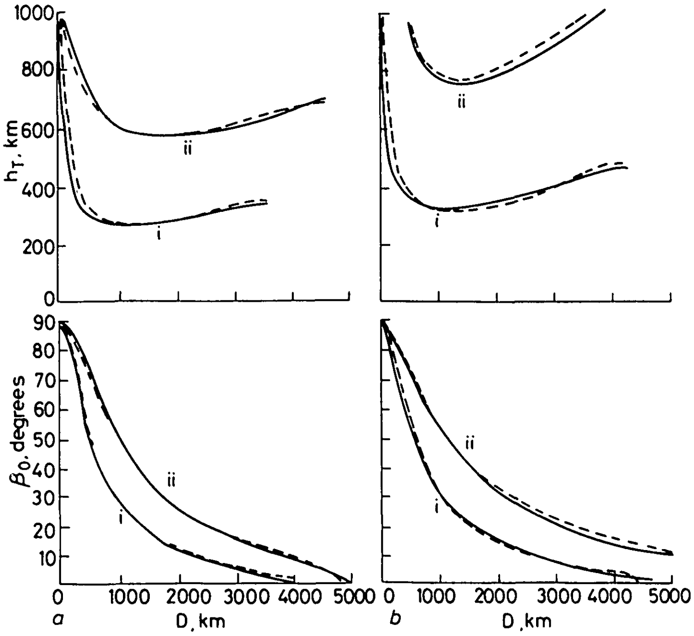

Fig. 14 *Fully calculated values and approximate estimates given by eqns. 16–21 ($r = 1.0$) for the mirror-reflection height, h_T, and elevation angle, β_0, as a function of distance, D*

a $x = 10.0$
b $x = 2.22$
i *hm*F2 = 250 km
ii *hm*F2 = 500 km
——— calculated values
- - - - estimates

6 Conclusions

From the results of ordinary-wave ray tracing through the Bradley–Dudeney model ionospheric profile using the Milsom equations, simple noniterative algorithms for rapid evaluation of mirror-reflection height have been developed. Algorithms of various complexity and accuracy are presented for the range of signal frequencies between 0.75 and 0.95 of the basic MUF. In addition, a single algorithm is given for a frequency equal to the basic MUF.

The most rigorous equations derived allow for the variation of mirror-reflection height with distance, M(3000)F2 and x, the ratio of the F- and E-layer critical frequencies; hence, all the required ionospheric inputs to the algorithm are scaled routinely from ionograms. No explicit dependence on signal frequency is included, but the equation for 0.75 to 0.95 times the basic MUF is accurate to within 6% for $x \geqslant 2.5$ and 11% for $x \geqslant 2.0$.

This accuracy involves considerable complexity, as compared with the widely used equation of Shimazaki which only allows for the variation with M(3000)F2 and has no dependence on distance or underlying ionisation; consequently, the Shimazaki equation is only accurate to within 34% for $x \geqslant 2.5$ and 45% for $x \geqslant 2.0$. For large x the full equation reduces to a comparable form to that of Shimazaki and is about 2% more accurate at all x. Such an equation may be sufficiently accurate at night, when x is large, but gives large errors by day when x is smaller. A second special case of the full equation ($x = 3$) leads to an expression with a non-negligible distance term which can be applied to day conditions with errors about 10% lower than those using the Shimazaki equation.

The algorithm presented for evaluation of mirror-reflection height for a signal frequency equal to the basic MUF yields values accurate to within 6% for $x \geqslant 2.5$. This is of comparable accuracy to the lower frequency algorithm, but the largest errors rise to 32% for cases where the elevation angle falls below a few degrees and x is between 2.0 and 2.5.

7 Acknowledgments

This work was carried out at the Rutherford Appleton Laboratory of the Science & Engineering Research Council as part of the Departmental Users Radio Propagation Programme. The author wishes to thank Mr P.A. Bradley who suggested the investigation and provided useful discussions.

8 References

1 CCIR: 'Second CCIR computer-based interim method for estimating sky-wave field strength and transmission loss at frequencies between 2 and 30 MHz'. Supplement to Report 252-2, 1978

2 BARGHAUSEN, A.F., FINNEY, J.W., PROCTOR, L.L., and SHULTZ, L.D.: 'Predicting long-term operational parameters of high-frequency sky-wave telecommunication systems'. ESSA Technical Report 110-ITS 78, USA Government Printing Office, Washington, 1969

3 SHIMAZAKI, T.: 'World-wide daily variations in the height of the maximum electron density of the ionospheric F2 layer', *J. Radio Res. Labs.*, 1955, **2**, pp. 85–97

4 APPLETON, E.V., and BEYNON, W.J.G.: 'The application of ionospheric data to radio communication problems', *Proc. Phys. Soc. (Pt. I)*, 1940, **52**, pp. 518–533

5 BOOKER, H.G., and SEATON, S.L.: 'Relation between actual and virtual ionospheric height', *Phys. Rev.*, 1940, **57**, pp. 87–94

6 SMITH, N.: 'The relation of radio skywave transmission to ionosphere measurements', *Proc. Inst. Radio Eng.*, 1939, **27**, pp. 332–345

7 WRIGHT, J.W., and McDUFFIE, R.E.: 'The relation of h_{max}F2 to M(3000)F2 and h_tF2', *J. Radio Res. Labs.*, 1960, **7**, pp. 409–419

8 CCIR: 'Propagation prediction methods for high frequency broadcasting'. Report 894, 1983

9 BRADLEY, P.A., and DUDENEY, J.R.: 'A simple model of the vertical distribution of electron concentration in the ionosphere', *J. Atmos. Terr. Phys.*, 1973, **35**, pp. 2131–2141

10 MILSON, J.D.: 'Exact ray-tracing through the Bradley–Dudeney model ionosphere', *Marconi Rev.*, 1977, **40**, pp. 172–196

11 LOCKWOOD, M.: 'Simple M-factor algorithm for improved estimation of the basic maximum usable frequency of radio waves reflected from the ionospheric F-region', *IEE Proc. F., Commun., Radar & Signal Process.*, 1983, **130**, pp. 296–302